Solvent exposure of Tyr10 as a probe of structural differences between monomeric and aggregated forms of the amyloid-β peptide

Biochemical and Biophysical Research Communications 468 (2015) 696–701

Contents lists available at ScienceDirect

Biochemical and Biophysical Research Communications

journal homepage: www.elsevier.com/locate/ybbrc

Solvent exposure of Tyr10 as a probe of structural differences between monomeric and aggregated forms of the amyloid-β peptide

Pablo Aran Terol [a], Janet R. Kumita [a], Sharon C. Hook [a, 1], Christopher M. Dobson [a], Elin K. Esbjörner [a, b, *]

[a] Department of Chemistry, University of Cambridge, Lensfield Road, Cambridge, CB2 1EW, UK
[b] Department of Biology and Biological Engineering, Division of Chemical Biology, Chalmers University of Technology, Kemivägen 10, 412 96 Gothenburg, Sweden

ARTICLE INFO

Article history:
Received 30 October 2015
Accepted 3 November 2015
Available online 10 November 2015

Keywords:
Amyloid-β
Aβ oligomer
Amyloid fibril
tyrosine fluorescence
Acrylamide quenching

ABSTRACT

Aggregation of amyloid-β (Aβ) peptides is a characteristic pathological feature of Alzheimer's disease. We have exploited the relationship between solvent exposure and intrinsic fluorescence of a single tyrosine residue, Tyr_{10}, in the Aβ sequence to probe structural features of the monomeric, oligomeric and fibrillar forms of the 42-residue $Aβ_{1-42}$. By monitoring the quenching of Tyr_{10} fluorescence upon addition of water-soluble acrylamide, we show that in $Aβ_{1-42}$ oligomers this residue is solvent-exposed to a similar extent to that found in the unfolded monomer. By contrast, Tyr_{10} is significantly shielded from acrylamide quenching in $Aβ_{1-42}$ fibrils, consistent with its proximity to the fibrillar cross-β core. Furthermore, circular dichroism measurements reveal that $Aβ_{1-42}$ oligomers have a considerably lower β-sheet content than the $Aβ_{1-42}$ fibrils, indicative of a less ordered molecular arrangement in the former. Taken together these findings suggest significant differences in the structural assembly of oligomers and fibrils that are consistent with differences in their biological effects.

1. Introduction

Alzheimer's disease (AD) and a range of related disorders are associated with the self-assembly, aggregation, and fibril formation of disease-specific peptides and proteins [1]; in the case of AD such processes are involved with aggregation of the amyloid-β (Aβ) peptide [2,3]. In its fibrillar form, this peptide is the main proteinaceous component of the extracellular plaque deposits that are characteristic of AD pathology [4,5], but in the brain Aβ also exists in a variety of monomeric and oligomeric forms [6]. It has been reported that soluble Aβ concentrations correlate more closely with dementia than the amount of amyloid plaques [7,8], and indeed soluble Aβ oligomers are now thought to be the main culprits in the pathogenesis of AD and related conditions [9], particularly since they have been associated with impaired cognitive function [10–12] and have been shown to induce cellular toxicity [13–17]. Unfortunately, the small size and low abundance of Aβ oligomers, in combination with their considerable heterogeneity and high sensitivity to environmental changes, has rendered them challenging to characterise. Although a detailed molecular model of a stabilised $Aβ_{1-42}$ protofibril has been recently reported [18], little is known in detail how monomers arrange to build up the smaller, globular oligomers that are populated during Aβ aggregation reactions and which can form in the AD brain [19].

In the present paper we have used fluorescence and circular dichroism spectroscopies to examine structural differences, particularly related to the microenvironment around the N-terminal region, to compare soluble, globular $Aβ_{1-42}$ oligomers, prepared *in vitro*, with monomers and fibrils formed by both $Aβ_{1-40}$ and $Aβ_{1-42}$. The oligomers were prepared using established methods for producing stable oligomers of a type that is often referred to as amyloid-derived diffusible ligands (ADDLs) [19]. These ADDLs have been reported to be neurotoxic [20] and it has been found that antibodies raised against *in vitro* prepared oligomers of this type also recognise oligomeric species that are elevated in AD brains [21], suggesting their resemblance to naturally occurring forms. Although it has been proposed that oligomers of this type could be of a fibrillar nature [22,23], it is not known how monomers are present within these oligomer assemblies or to what extent the

* Corresponding author. Department of Biology and Biological Engineering, Division of Chemical Biology, Chalmers University of Technology, Kemivägen 10, 412 96 Gothenburg, Sweden.
E-mail address: eline@chalmers.se (E.K. Esbjörner).
[1] Present address: School of Biochemistry, University Walk, University of Bristol, Bristol, BS8 1TD, UK.

http://dx.doi.org/10.1016/j.bbrc.2015.11.018

microscopic architecture resembles that found in mature fibrils. To address this issue, we have taken advantage of the fact that the Aβ peptide contains only a single intrinsically fluorescent residue, tyrosine at position 10 (Tyr_{10}), which is located in between the β-core and the flexible N-terminus of fibrillar $Aβ_{1-40}$ and $Aβ_{1-42}$ [24–28] (Fig. 1A). This residue, therefore, has the potential to report on the participation of this region of the Aβ peptide in the different aggregated states. In this study, we have exploited the intrinsic fluorescent properties of Tyr_{10} and also its susceptibility to fluorescence quenching by water-soluble acrylamide to examine the characteristics of the monomeric, oligomeric and fibrillar forms of Aβ. Our results indicate that $Aβ_{1-42}$ oligomers show the presence of a degree of β-sheet structure, but that they are distinctly less ordered than fibrils, and this is confirmed by a substantially higher degree of solvent exposure around Tyr_{10}. Taken together these results highlight significant differences in the molecular architecture of the oligomeric versus the fibrillar forms of the Aβ peptides which may offer new insights into the differential biological activities.

2. Materials and methods

2.1. Materials

Synthetic $Aβ_{1-40}$ and $Aβ_{1-42}$ peptides were acquired as lyophilised powders from Anaspec EGT (Fremont, USA) and were prepared for use as described below. All other reagents were purchased from Sigma–Aldrich (Dorset, UK).

2.2. Sample preparation

The Aβ peptide powders were dissolved in ice-cold trifluoroacetic acid, sonicated (30 s, on ice), flash frozen and again lyophilised. The samples were redissolved in ice-cold hexafluoroisopropanol (1 mL) and the solutions were kept on ice (10 min) then divided into aliquots (50 μL) whilst working at 4 °C, and dried by rotary evaporation. The peptide concentration was determined by amino acid analysis and all experiments were performed in 50 mM sodium phosphate buffer (pH 7.4). The monomeric form of the Aβ peptides was obtained by dissolving a fresh peptide aliquot to a final concentration of 5 μM directly in buffer. The solution was analysed immediately to minimise the formation of aggregates. Fibrillar Aβ samples were prepared by incubation at room temperature for 48 h under shaking conditions (1400 rpm in a Titramax 100 shaker, Heidolph Instruments GmbH, Schwabach, Germany). Oligomers of $Aβ_{1-42}$ were prepared by resuspending peptide aliquots in DMSO (2 μL), followed by dilution in ice-cold buffer (10 mM NaCl, 10 mM sodium phosphate, pH 7.4), to a final peptide concentration of 100 μM followed by incubation (overnight, 4 °C under quiescent conditions) [20]. The solutions were diluted in 50 mM sodium phosphate buffer (pH 7.4) (5 μM based on

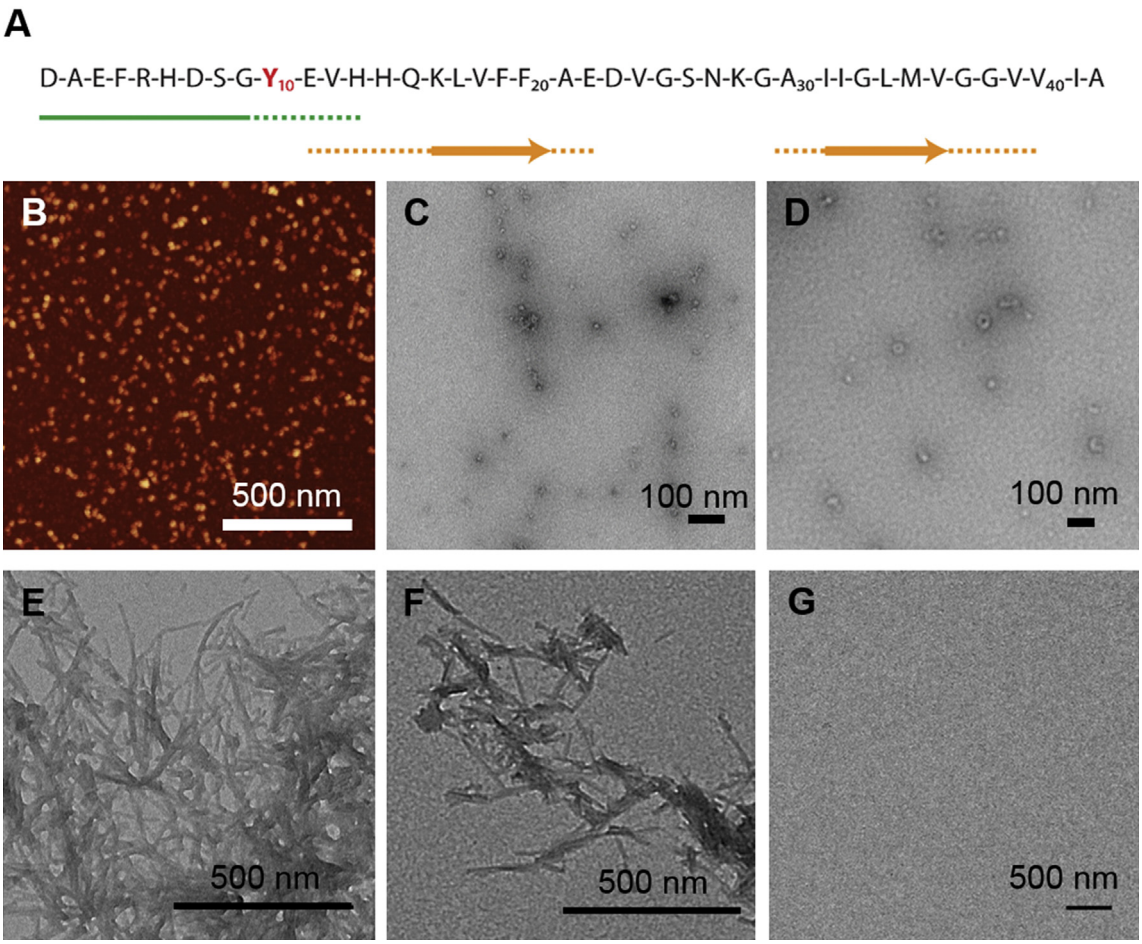

Fig. 1. (A) Schematic representation of the $Aβ_{1-42}$ peptide sequence. The arrows show the reported engagement of different parts of the sequence in the mature amyloid fibrils [24–28], with the unstructured N-terminus marked in green and the β-sheet regions participating in the core marked in orange. Tyr_{10} is highlighted in red. (B) Atomic force microscopy image of $oAβ_{1-42}$. (C–D) TEM image of $oAβ_{1-42}$ at higher magnification. (E) TEM image of $fAβ_{1-40}$. (F) TEM image of $fAβ_{1-42}$. (G) TEM image of $mAβ_{1-40}$ showing the absence of aggregates in the monomeric preparation. (For interpretation of the references to colour in this figure legend, the reader is referred to the web version of this article.)

monomer concentration) prior to experimental analysis. The oligomer yield was determined by amino acid analysis following separation of the oligomers from residual monomer by ultracentrifugation (1 h, 90,000 g) using an Optima TLX ultracentrifuge (Beckman Coulter Inc, Brea, USA).

2.3. Fluorescence spectroscopy

Fluorescence spectra were recorded on a Cary Eclipse fluorimeter (Agilent Technologies, Stockport, UK) using a reduced pathlength quartz cuvette (4 mm excitation/10 mm emission). The excitation wavelength was 275 nm and emission spectra were recorded at 1 nm increments between 290 and 350 nm, with excitation and emission slit widths of 5 nm and 10 nm, respectively, and a scan rate of 60 nm/min. Samples were subjected to an acrylamide gradient following additions of a 0.2 M stock solution (10 μL aliquots), the fluorescence spectra being recorded immediately after the addition of the acrylamide aliquots. The recorded spectra were corrected for the background contributions and the fluorescence intensity in each case was taken as the sum of the intensities in a 6 nm range centred around the emission maxima, to increase signal-to-noise. Data were analysed using the Stern-Volmer equation [29].

$$\frac{F_0}{F} = 1 + K_{SV}[Q] \quad (1)$$

where F_0 and F are the fluorescence intensities in the absence and presence of quencher, [Q] is the concentration of quencher, and K_{SV} the Stern–Volmer constant. All experiments were performed in triplicate and are reported as mean ± SD. As acrylamide absorbs significantly at the excitation wavelength of tyrosine and therefore acts as an inner filter, corrections were made using separate experiments in which a non-quenching molecule (here DNA) was titrated into solutions of tyrosine at the same absorbance increments in order to determine correction factors for primary inner filter effects.

2.4. Circular dichroism (CD) spectroscopy

CD spectra were recorded on a JASCO J-810 spectropolarimeter (JASCO Inc. Tokyo, Japan) between 190 and 250 nm using a 1 mm quartz cuvette. 10 scans were recorded and averaged using a bandwidth of 2 nm and a scan speed of 50 nm/min. The peptide concentration was 30 μM and all spectra were corrected for background contributions by subtracting buffer blanks.

2.5. Transmission electron microscopy (TEM)

Aβ samples were adsorbed (2 min) onto carbon-coated copper grids (Taab Laboratories Equipment Ltd, Berks, UK). The grids were blotted, washed with milliQ water (2X) and negatively stained with 2% (w/v) uranyl acetate. Samples were imaged on a FEI Tecnai G2 transmission electron microscope (Eindhoven, Netherlands) and images were analysed using the SIS Megaview II Image Capture system (EMSIS GmbH, Muenster, Germany).

2.6. Atomic force microscopy (AFM)

AFM measurements were performed using a NanoWizard AFM system (JPK Instruments AG, Berlin, Germany). Samples were diluted using dH_2O and deposited onto freshly cleaved mica surfaces and slowly dried before imaging. AFM imaging was carried out in the intermittent (air) contact mode using a silicon nitride cantilever (μmasch, NSC36/No Al, 65–130 kHz, 0.6–2 N/m). AFM images were analysed using Gwyddion software package (http://gwyddion.net/).

3. Results and discussion

The intrinsic fluorescence of Tyr_{10} in combination with circular dichroism spectroscopy has been used to examine five different preparations of $A\beta_{1\text{-}40}$ and $A\beta_{1\text{-}42}$; monomers ($mA\beta_{1\text{-}40}$ and $mA\beta_{1\text{-}42}$), fibrils ($fA\beta_{1\text{-}40}$ $fA\beta_{1\text{-}42}$) and $A\beta_{1\text{-}42}$ oligomers ($oA\beta_{1\text{-}42}$) in order to assess the conformational differences between the various forms of $A\beta_{1\text{-}42}$, and also to explore potential differences between $A\beta_{1\text{-}40}$ and $A\beta_{1\text{-}42}$ fibrils.

Prior to spectroscopic characterisation the morphology of the different Aβ species was examined (Fig. 1B–G). Analysis of the oligomeric $oA\beta_{1\text{-}42}$ samples by AFM (Fig. 1B) and TEM (Fig. 1C–D) showed that they contain a relatively homogeneous population of small aggregates with approximately spherical morphology; analysis of the TEM images indicates that their approximate diameters were 10–20 nm. The fibrillar $fA\beta_{1\text{-}40}$ and $fA\beta_{1\text{-}42}$ samples contained typical amyloid fibrils; importantly no such fibrillar structures were detected in the oligomeric samples used in this study and no discernible aggregates were observed in the monomeric samples (Fig. 1G,).

Next, the secondary structure content in the different Aβ preparations was assessed (Fig. 2); the monomeric samples displayed CD spectra typical of random coils with negative peaks centred at 195 nm, consistent with their intrinsically disordered nature and confirming the absence of amyloid aggregates in the monomer preparations. The oligomeric and fibrillar samples, by contrast, exhibited characteristic β-sheet features with CD spectra displaying a negative peak at ~218 nm and a positive peak at ~196 nm. The CD signal from the oligomers, however, was considerably weaker than that of the fibrils indicating that they have significantly less β-sheet content.

The fluorescence spectra of the various Aβ samples were recorded to monitor the intrinsic emission from Tyr_{10}. Fig. 3A shows the spectra of the five different Aβ preparations along with corresponding spectra for free tyrosine and for a tyrosine-containing tri-peptide (VYV), the latter was used to determine the generic effects on tyrosine emission due to its incorporation into a polypeptide sequence. It was observed that the tyrosine emission intensity is decreased by as much as a factor of 2 upon incorporation into a peptide sequence, consistent with previous observations where the quenching of tyrosine in proteins has been attributed to photoinduced electron transfer to the peptide bond in presence of electron withdrawing groups [30]. All the Aβ conformers examined, except $fA\beta_{1\text{-}42}$, were observed to exhibit even lower intrinsic tyrosine fluorescence intensities than the VYV

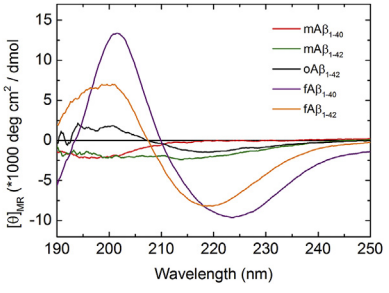

Fig. 2. Circular dichroism spectra of different Aβ species; mAβ1-40 (red), $mA\beta_{1\text{-}42}$ (green), $oA\beta_{1\text{-}42}$ (black), $fA\beta_{1\text{-}40}$ (purple) and $fA\beta_{1\text{-}42}$ (orange). (For interpretation of the references to colour in this figure legend, the reader is referred to the web version of this article.)

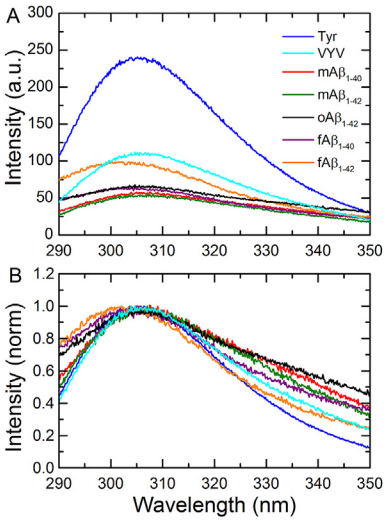

Fig. 3. Intrinsic tyrosine fluorescence of different Aβ species. (A) Emission spectra of free tyrosine (blue), VYV (cyan), $mA\beta_{1\text{-}40}$ (red), $mA\beta_{1\text{-}42}$ (green), $oA\beta_{1\text{-}42}$ (black), $fA\beta_{1\text{-}40}$ (purple), $fA\beta_{1\text{-}42}$ (orange). (B) Normalised emission intensity, corresponding to the spectra shown in (A). (For interpretation of the references to colour in this figure legend, the reader is referred to the web version of this article.)

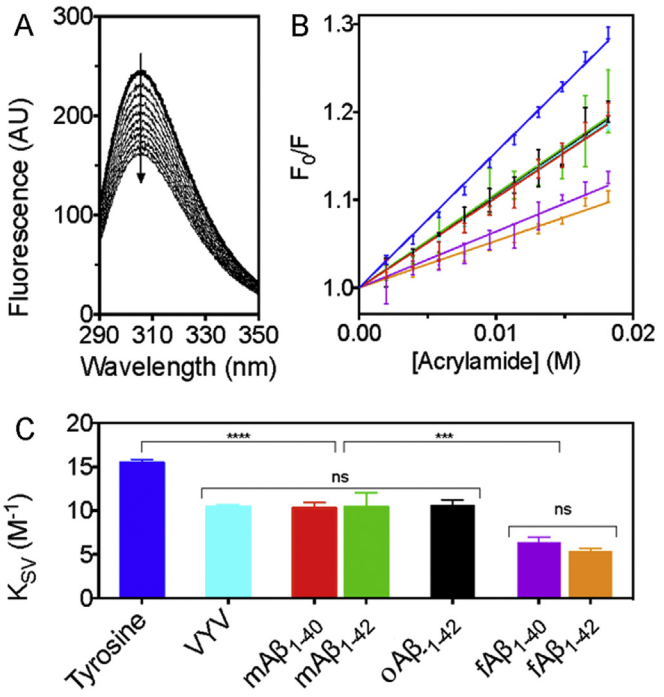

Fig. 4. Acrylamide quenching of the intrinsic tyrosine fluorescence in the different species of Aβ. (A) Fluorescence emission spectra for free tyrosine (5 μM) titrated with acrylamide (added in 2 mM increments). The bold line represents the fluorescence of unquenched tyrosine and the arrow indicates the decrease in fluorescence with increasing concentration of the quencher. (B) Stern-Volmer plots of the acrylamide quenching of Tyr_{10} in the different Aβ species showing free tyrosine (blue), VYV (cyan), $mA\beta_{1\text{-}40}$ (red), $mA\beta_{1\text{-}42}$ (green), $oA\beta_{1\text{-}42}$ (black) $fA\beta_{1\text{-}40}$ (purple), $fA\beta_{1\text{-}42}$ (orange). The error bars represent the standard deviations (n = 3). (C) Stern–Volmer quenching constants (K_{SV}) ±SD calculated from the linear-fit of the data in (B). The statistical significance of the differences between the various K_{SV} values was tested by one-way ANOVA with Tukey's post hoc test; *ns* denotes not significantly different ($p > 0.05$), *** ($p < 0.001$), **** ($p < 0.0001$). (For interpretation of the references to colour in this figure legend, the reader is referred to the web version of this article.)

control peptide, indicating the existence of additional quenching interactions within the Aβ sequence, attributable to interactions with neighbouring side-chains. Spectral broadening of the tyrosine emission peak was observed in all the Aβ samples (Fig. 3B); the broadening on the blue edge of the emission peak is particularly apparent for $fA\beta_{1\text{-}40}$, $fA\beta_{1\text{-}42}$ and $oA\beta_{1\text{-}42}$ and can be explained by light scattering by the aggregates present in these solutions, whereas the red edge broadening, which is mainly apparent for the monomeric Aβ peptides, may be indicative of tyrosinate formation in the excited state [31,32].

Acrylamide quenching experiments were conducted to explore the extent to which tyrosine is exposed to solvent in its free form (Fig. 4A) compared to its exposure when it is incorporated as Tyr_{10} in the different monomeric and aggregated forms of Aβ. The resulting Stern-Volmer plots (Fig. 4B) were linear in all cases, an observation consistent with acrylamide being a predominately collisional quencher [33]. Fig. 4C summarises the calculated Stern–Volmer quenching constants (K_{SV}) and shows that incorporation of tyrosine into a peptide sequence, even into the short VYV model peptide which displays a ~30% reduction of the K_{SV} value, results in shielding from the polar but non-charged water soluble acrylamide quencher. This effect is likely to be due to steric hindrance imparted by the neighbouring residues, which limits the number of possible quenching interactions but does not reflect shielding caused by secondary structure constraints. No appreciable differences in the solvent exposure of tyrosine in the monomeric $mA\beta_{1\text{-}40}$ and $mA\beta_{1\text{-}42}$ forms compared to the VYV peptide were observed. This finding is consistent with other observations showing that the Aβ chain is highly unfolded in solution [34,35], at least on timescales in the order of the excited state lifetime of tyrosine (≤3.4 ns [36]). Analysis of the Stern-Volmer plots showed, however, that Tyr_{10} in $fA\beta_{1\text{-}40}$ and $fA\beta_{1\text{-}42}$ is considerably less exposed to acrylamide quenching than in $mA\beta_{1\text{-}40}$ and $mA\beta_{1\text{-}42}$, suggesting that the incorporation of the Aβ molecules into a fibrillar structure protects this residue from solvent even though existing structural models [24–28] suggest that Tyr_{10} does not participate directly in the cross-β core (see summary in Fig. 1). This effect can, however, be explained by the close packing of monomer units in the fibril protofilaments [37], which sterically hinders the acrylamide-Tyr_{10} collisions, or it may also be a consequence of a fraction of the Aβ N-termini becoming buried within the mature fibril; indeed, limited proteolysis data for $fA\beta_{1\text{-}40}$ suggests that at least 20% of Aβ monomers have an N-terminal segment that is protected within the fibril structure [38]. The considerable similarity observed for $fA\beta_{1\text{-}40}$ and $fA\beta_{1\text{-}42}$ is interesting in relation to hydrogen/deuterium-exchange rates measured by NMR, which indicate significant differences between the two fibril types with respect to the amide solvent protection of the N-terminus, whereby the amide group of Tyr_{10} is more solvent accessible in $fA\beta_{1\text{-}42}$ than in $fA\beta_{1\text{-}40}$ [26].

Interestingly, the oligomeric $oA\beta_{1\text{-}42}$ samples exhibit K_{SV} values that are significantly higher than those observed for the fibrils (Fig. 4C). This observation suggests that Tyr_{10} is considerably less shielded in these globular oligomers than in Aβ fibrils and is consistent with our finding that $oA\beta_{1\text{-}42}$ species have a lower β-sheet content than $fA\beta_{1\text{-}42}$ (Fig. 2A). More surprisingly, we also find that the K_{SV} values of the oligomers are similar, within experimental error, to those of monomeric Aβ implying that Tyr_{10} is exposed to a similar extent as in a random coil monomer. To ensure that the high K_{SV} value truly reflects the structure of the $oA\beta_{1\text{-}42}$ species and is not attributable to sample heterogeneity, and as it has been suggested previously that oligomers of the type we examine here can exist in binary mixtures with monomers, a further control experiment was performed [39]. Quantitative amino acid analysis following ultracentrifugation to separate the

oA$\beta_{1\text{-}42}$ species from residual monomers showed that, in our samples, nearly 90% of the Aβ monomers were incorporated into oligomers (Supplementary Information). This result is comparable to our previous report of the yield in fibril forming reactions with A$\beta_{1\text{-}40}$ and A$\beta_{1\text{-}42}$ [40]. Furthermore, these control experiments confirm that the difference in β-sheet content indicated in the oA$\beta_{1\text{-}42}$ and fA$\beta_{1\text{-}42}$ CD spectra, is indeed related to the oA$\beta_{1\text{-}42}$ species exhibiting some random coil nature, rather than due to the presence of significant quantities of unstructured monomers in the samples. Therefore, this study shows that the A$\beta_{1\text{-}42}$ oligomers differ from fA$\beta_{1\text{-}42}$, not only in size and shape, but also in secondary structure content and internal architecture. Our finding that Tyr10 in the oligomers is significantly solvent exposed, and thus likely to be present on the surface of the oligomers is in agreement with a previous study of a disc shaped A$\beta_{1\text{-}42}$ pentamer [41]. These observations are also consistent with the conclusion that the A$\beta_{1\text{-}42}$ peptides in these oligomers do not adopt the same β-hairpin arrangement as that formed in the mature Aβ fibrils. This suggestion supports the idea that oligomers of this type may accumulate because their structural properties are such that they are not able to convert into fibrils [42,43].

In conclusion, this study has set out to examine the fluorescent properties and the degree of solvent exposure of Tyr_{10} in Aβ to gain insights into structural similarities and dissimilarities between different Aβ species. We report significant differences between monomers and fibrils, suggesting that even though Tyr_{10} is not directly part of the cross-β core, the side-chain is, on average, well shielded within the fibrils. In addition, we have shown that A$\beta_{1\text{-}42}$ oligomers, due to their lower β-sheet content and extensive exposure of Tyr_{10} to solvent, have significantly different structural properties from those of Aβ fibrils.

Acknowledgements

This work was funded by grants to E.K.E from the Wenner-Gren Foundations, the Hasselblad Foundation, and the Swedish Innovation Agency (Vinnova): 2011-03488 and to C.M.D from the Wellcome Trust. The TEM imaging was carried out in the Multi-Imaging Unit in the Department of Physiology, Development and Neuroscience, University of Cambridge, UK and quantitative amino acid analysis was carried out at the Protein and Nucleic Acid Chemistry Facility, Department of Biochemistry, University of Cambridge, UK.

Appendix A. Supplementary data

Supplementary data related to this article can be found at http://dx.doi.org/10.1016/j.bbrc.2015.11.018.

Transparency document

Transparency document related to this article can be found online at http://dx.doi.org/10.1016/j.bbrc.2015.11.018.

References

[1] F. Chiti, C.M. Dobson, Protein misfolding, functional amyloid, and human disease, Annu. Rev. Biochem. 75 (2006) 333–366.
[2] J. Hardy, D. Allsop, Amyloid deposition as the central event in the aetiology of Alzheimer's disease, Trends Pharmacol. Sci. 12 (1991) 383–388.
[3] J.A. Hardy, G.A. Higgins, Alzheimer's disease: the amyloid cascade hypothesis, Science 256 (1992) 184–185.
[4] G.G. Glenner, C.W. Wong, Alzheimer's disease: initial report of the purification and characterization of a novel cerebrovascular amyloid protein, Biochem. Biophys. Res. Commun. 120 (1984) 885–890.
[5] C.L. Masters, G. Simms, N.A. Weinman, G. Multhaup, B.L. McDonald, K. Beyreuther, Amyloid plaque core protein in Alzheimer disease and Down syndrome, Proc. Natl. Acad. Sci. U. S. A. 82 (1985) 4245–4249.
[6] C.G. Glabe, Structural classification of toxic amyloid oligomers, J. Biol. Chem. 283 (2008) 29639–29643.
[7] L.F. Lue, Y.M. Kuo, A.E. Roher, L. Brachova, Y. Shen, L. Sue, T. Beach, J.H. Kurth, R.E. Rydel, J. Rogers, Soluble amyloid beta peptide concentration as a predictor of synaptic change in Alzheimer's disease, Am. J. Pathol. 155 (1999) 853–862.
[8] C.A. McLean, R.A. Cherny, F.W. Fraser, S.J. Fuller, M.J. Smith, K. Beyreuther, A.I. Bush, C.L. Masters, Soluble pool of Abeta amyloid as a determinant of severity of neurodegeneration in Alzheimer's disease, Ann. Neurol. 46 (1999) 860–866.
[9] C. Haass, D.J. Selkoe, Soluble protein oligomers in neurodegeneration: lessons from the Alzheimer's amyloid beta-peptide, Nat. Rev. Mol. Cell Biol. 8 (2007) 101–112.
[10] J.P. Cleary, D.M. Walsh, J.J. Hofmeister, G.M. Shankar, M.A. Kuskowski, D.J. Selkoe, K.H. Ashe, Natural oligomers of the amyloid-beta protein specifically disrupt cognitive function, Nat. Neurosci. 8 (2005) 79–84.
[11] S. Lesne, M.T. Koh, L. Kotilinek, R. Kayed, C.G. Glabe, A. Yang, M. Gallagher, K.H. Ashe, A specific amyloid-beta protein assembly in the brain impairs memory, Nature 440 (2006) 352–357.
[12] D.J. Selkoe, Soluble oligomers of the amyloid beta-protein impair synaptic plasticity and behavior, Behav. Brain Res. 192 (2008) 106–113.
[13] S. Campioni, B. Mannini, M. Zampagni, A. Pensalfini, C. Parrini, E. Evangelisti, A. Relini, M. Stefani, C.M. Dobson, C. Cecchi, F. Chiti, A causative link between the structure of aberrant protein oligomers and their toxicity, Nat. Chem. Biol. 6 (2010) 140–147.
[14] B. Bolognesi, J.R. Kumita, T.P. Barros, E.K. Esbjörner, L.M. Luheshi, D.C. Crowther, M.R. Wilson, C.M. Dobson, G. Favrin, J.J. Yerbury, ANS binding reveals common features of cytotoxic amyloid species, ACS Chem. Biol. 5 (2010) 735–740.
[15] K.N. Dahlgren, A.M. Manelli, W.B. Stine Jr., L.K. Baker, G.A. Krafft, M.J. LaDu, Oligomeric and fibrillar species of amyloid-beta peptides differentially affect neuronal viability, J. Biol. Chem. 277 (2002) 32046–32053.
[16] A. Sandberg, L.M. Luheshi, S. Söllvander, T.P. Barros, B. Macao, T.P.J. Knowles, H. Biverståhl, C. Lendel, F. Ekholm-Petterson, A. Dubnovitsky, L. Lannfelt, C.M. Dobson, T. Härd, Stabilization of neurotoxic Alzheimer amyloid-β oligomers by protein engineering, Proc. Natl. Acad. Sci. U. S. A. 107 (2010) 15595–15600.
[17] D.M. Walsh, I. Klyubin, J.V. Fadeeva, W.K. Cullen, R. Anwyl, M.S. Wolfe, M.J. Rowan, D.J. Selkoe, Naturally secreted oligomers of amyloid beta protein potently inhibit hippocampal long-term potentiation in vivo, Nature 416 (2002) 535–539.
[18] C. Lendel, M. Bjerring, A. Dubnovitsky, R.T. Kelly, A. Filippov, O.N. Antzutkin, N.C. Nielsen, T. Hard, A hexameric peptide barrel as building block of amyloid-beta protofibrils, Angew. Chem. Int. Ed. 53 (2014) 12756–12760.
[19] P. Narayan, A. Orte, R.W. Clarke, B. Bolognesi, S. Hook, K.A. Ganzinger, S. Meehan, M.R. Wilson, C.M. Dobson, D. Klenerman, The extracellular chaperone clusterin sequesters oligomeric forms of the amyloid-beta(1-40) peptide, Nat. Struct. Mol. Biol. 19 (2012) 79–83.
[20] M.P. Lambert, A.K. Barlow, B.A. Chromy, C. Edwards, R. Freed, M. Liosatos, T.E. Morgan, I. Rozovsky, B. Trommer, K.L. Viola, P. Wals, C. Zhang, C.E. Finch, G.A. Krafft, W.L. Klein, Diffusible, nonfibrillar ligands derived from Abeta1-42 are potent central nervous system neurotoxins, Proc. Natl. Acad. Sci. U. S. A. 95 (1998) 6448–6453.
[21] Y. Gong, L. Chang, K.L. Viola, P.N. Lacor, M.P. Lambert, C.E. Finch, G.A. Krafft, W.L. Klein, Alzheimer's disease-affected brain : presence of oligomeric Abeta ligands (ADDLs) suggests a molecular basis for reversible memory loss, Proc. Natl. Acad. Sci. U. S. A. 100 (2003) 10417–10422.
[22] P.N. Lacor, M.C. Buniel, L. Chang, S.J. Fernandez, Y. Gong, K.L. Viola, M.P. Lambert, P.T. Velasco, E.H. Bigio, C.E. Finch, G.A. Krafft, W.L. Klein, Synaptic targeting by Alzheimer's-related amyloid beta oligomers, J. Neurosci. 24 (2004) 10191–10200.
[23] M.P. Lambert, P.T. Velasco, L. Chang, K.L. Viola, S. Fernandez, P.N. Lacor, D. Khuon, Y. Gong, E.H. Bigio, P. Shaw, F.G. De Felice, G.A. Krafft, W.L. Klein, Monoclonal antibodies that target pathological assemblies of Abeta, J. Neurochem. 100 (2007) 23–35.
[24] M. Fandrich, M. Schmidt, N. Grigorieff, Recent progress in understanding Alzheimer's beta-amyloid structures, Trends Biochem. Sci. 36 (2011) 338–345.
[25] T. Luhrs, C. Ritter, M. Adrian, D. Riek-Loher, B. Bohrmann, H. Dobeli, D. Schubert, R. Riek, 3D structure of Alzheimer's amyloid-beta(1-42) fibrils, Proc. Natl. Acad. Sci. U. S. A. 102 (2005) 17342–17347.
[26] A. Olofsson, M. Lindhagen-Persson, A.E. Sauer-Eriksson, A. Ohman, Amide solvent protection analysis demonstrates that amyloid-beta(1-40) and amyloid-beta(1-42) form different fibrillar structures under identical conditions, Biochem. J. 404 (2007) 63–70.
[27] A. Olofsson, A.E. Sauer-Eriksson, A. Ohman, The solvent protection of Alzheimer amyloid-beta-(1-42) fibrils as determined by solution NMR spectroscopy, J. Biol. Chem. 281 (2006) 477–483.
[28] A.T. Petkova, Y. Ishii, J.J. Balbach, O.N. Antzutkin, R.D. Leapman, F. Delaglio, R. Tycko, A structural model for Alzheimer's beta-amyloid fibrils based on experimental constraints from solid state NMR, Proc. Natl. Acad. Sci. U. S. A. 99 (2002) 16742–16747.
[29] O. Stern, M. Volmer, Uber die Abklingzeit der Fluoreszenz, Z Phys. 20 (1919) 183–188.
[30] C. Seidel, A. Orth, K.O. Greulich, Electronic effects on the fluorescence of tyrosine in small peptides, Photochem. Photobiol. 58 (1993) 178–184.
[31] S. Pundak, R.S. Roche, Tyrosine and tyrosinate fluorescence of bovine testes

calmodulin: calcium and pH dependence, Biochemistry 23 (1984) 1549–1555.
[32] A.G. Szabo, K.R. Lynn, D.T. Krajcarski, D.M. Rayner, Tyrosinate fluorescence maxima at 345 nm in proteins lacking tryptophan at pH 7, FEBS Lett. 94 (1978) 249–252.
[33] M.R. Eftink, C.A. Ghiron, Exposure of tryptophanyl residues in proteins. Quantitative determination by fluorescence quenching studies, Biochemistry 15 (1976) 672–680.
[34] J. Danielsson, A. Andersson, J. Jarvet, A. Gräslund, 15N relaxation study of the amyloid beta-peptide: structural propensities and persistence length, Magn. Reson. Chem. 44 (2006) S114–S121.
[35] R. Riek, P. Guntert, H. Dobeli, B. Wipf, K. Wuthrich, NMR studies in aqueous solution fail to identify significant conformational differences between the monomeric forms of two Alzheimer peptides with widely different plaque-competence, A beta(1-40)(ox) and A beta(1-42)(ox), Eur. J. Biochem. 268 (2001) 5930–5936.
[36] J.B.A. Ross, W.R. Laws, K.W. Rousslang, H.R. Wyssbrod, Tyrosine Fluorescence and Phosphorescence from Proteins and Polypeptides, in: J. Lakowicz (Ed.), Topics in Fluorescence Spectroscopy, Biochemical Applications, vol. 3, Plenum Press, New York, 1992, pp. 1–63.
[37] L.C. Serpell, Alzheimer's amyloid fibrils: structure and assembly, BBA Mol. Bas. Dis. 1502 (2000) 16–30.
[38] I. Kheterpal, A. Williams, C. Murphy, B. Bledsoe, R. Wetzel, Structural features of the Abeta amyloid fibril elucidated by limited proteolysis, Biochemistry 40 (2001) 11757–11767.
[39] R.W. Hepler, K.M. Grimm, D.D. Nahas, R. Breese, E.C. Dodson, P. Acton, P.M. Keller, M. Yeager, H. Wang, P. Shughrue, G. Kinney, J.G. Joyce, Solution state characterization of amyloid beta-derived diffusible ligands, Biochemistry 45 (2006) 15157–15167.
[40] D.J. Lindberg, M.S. Wranne, M. Gilbert Gatty, F. Westerlund, E.K. Esbjörner, Steady-state and time-resolved Thioflavin-T fluorescence can report on morphological differences in amyloid fibrils formed by Abeta(1-40) and Abeta(1-42), Biochem. Biophys. Res. Commun. 458 (2015) 418–423.
[41] M. Ahmed, J. Davis, D. Aucoin, T. Sato, S. Ahuja, S. Aimoto, J.I. Elliott, W.E. Van Nostrand, S.O. Smith, Structural conversion of neurotoxic amyloid-beta(1-42) oligomers to fibrils, Nat. Struct. Mol. Biol. 17 (2010) 561–567.
[42] S.W. Chen, S. Drakulic, E. Deas, M. Ouberai, F.A. Aprile, R. Arranz, S. Ness, C. Roodveldt, T. Guilliams, E.J. De-Genst, D. Klenerman, N.W. Wood, T.P. Knowles, C. Alfonso, G. Rivas, A.Y. Abramov, J.M. Valpuesta, C.M. Dobson, N. Cremades, Structural characterization of toxic oligomers that are kinetically trapped during alpha-synuclein fibril formation, Proc. Natl. Acad. Sci. U. S. A. 112 (2015) E1994–E2003.
[43] M. Necula, R. Kayed, S. Milton, C.G. Glabe, Small molecule inhibitors of aggregation indicate that amyloid beta oligomerization and fibrillization pathways are independent and distinct, J. Biol. Chem. 282 (2007) 10311–10324.